BUTTERWORTH HEINEMANN

Polymer Vol. 36 No. 20, pp. 3831–3840, 1995

0032-3861/95/$10.00+0.00

Time-resolved synchrotron small angle X-ray scattering studies of poly(3-hydroxybutyrate) and poly(3-hydroxybutyrate-*co*-3-hydroxyvalerate) polymers

R. J. Rule*
ICI Chemicals & Polymers, Runcorn Technical Centre, The Heath, PO Box 8, Runcorn, Cheshire, WA7 4QD, UK

and J. J. Liggat
Zeneca Bio Products, PO Box 2, Billingham, Cleveland, TS23 1YN, UK
(Received 2 September 1994; revised 13 December 1994)

Time-resolved synchrotron small-angle X-ray scattering measurements have been performed during the heating and melting of poly(3-hydroxybutyrate) and poly(3-hydroxybutyrate-*co*-3-hydroxyvalerate). A rapid, continuous rise in *d*-spacing was observed during melting, consistent with the disappearance of thinner, unstable crystals from stacks of lamellae possessing a broad distribution of thicknesses. The thickening of the remaining crystals has been characterized during the annealing of a copolymer close to its melting temperature. Differential scanning calorimetry measurements have indicated the presence of multiple melting endotherms in the case of the copolymer but not in the homopolymer. These multiple endotherms have been related to the effects of the hydroxyvalerate units in limiting the thickness of the lamellae at any given temperature.

(Keywords: poly(3-hydroxybutyrate); X-ray scattering; structure)

INTRODUCTION

Poly(3-hydroxybutyrate) (PHB) and the random copolymers with 3-hydroxyvalerate (PHB–HV) are linear aliphatic polyester polymers manufactured and marketed by Zeneca Bio Products under the trade name 'Biopol'. The polymers possess the physical properties and processability of conventional thermoplastics yet are fully biodegradable when disposed of in a microbially active environment[1] and, as such, are finding an increasing number of applications in packaging and waste management[2].

PHB occurs naturally in a wide range of microorganisms which use it as an energy storage medium in the same manner that humans accumulate fat[3]. Industrially, the polymer is produced by the large-scale fermentation of the bacterium *Alcaligenes eutrophus* using glucose as the fermentation medium; adding controlled amounts of an organic acid to the medium encourages the production of the PHB–HV copolymer[4].

The polymers are completely stereoregular and therefore crystallize readily; crystallinities of 60–70% are achievable. This value remains essentially independent of HV content as, although slightly larger than HB units, the HV units can be accommodated in the HB lattice[5–7]. This phenomenon, and the complex melting behaviour of these polymers as observed by differential scanning calorimetry (d.s.c.), makes them particularly worthy of morphological study.

Small-angle X-ray scattering (SAXS) is a well established technique for probing the morphology of polymers and provides information describing structural features of the order of 10–1000 Å in size[8,9]. In samples possessing a regular, ordered morphology, a correlation peak is observed in the SAXS intensity at a characteristic value of q (denoted by q_{max}), which is related to the separation of domains or heterogeneities in the material. In the simplest analysis, the scattering may be treated according to Bragg's Law and hence:

$$q_{max} = 2\pi/d \qquad (1)$$

where d is the average interdomain spacing and q is the scattering vector, defined as $(4\pi \sin\theta)/\lambda$ where θ is the scattering angle and λ is the X-ray wavelength.

In the case of a semicrystalline polymer possessing a lamellar morphology (such as PHB and PHB–HV) which is isotropically distributed throughout the material, the Lorentz correction is applied to the SAXS intensity prior to the determination of the peak position. The

* To whom correspondence should be addressed. Present address: ICI Polyester, PO Box 90, Wilton Centre, Middlesbrough, Cleveland, TS90 8JE, UK

Lorentz correction involves the multiplication of the intensity function by a factor of q^2 and has the effect of shifting the position of a broad correlation peak to higher values of q.

According to the simple, ideal lamellar model used to describe certain semicrystalline synthetic polymers, the d-spacing represents the distance between adjacent crystalline lamellae which are separated by amorphous domains and arranged in space-filling stacks. The d-spacing is thus equivalent to the sum of the crystalline and amorphous layer thicknesses (l_c and l_a respectively):

$$d = l_c + l_a \tag{2}$$

An independent knowledge of the degree of crystallinity of the sample (ϕ_c) enables both of the above parameters to be estimated, assuming the lamellar stacks to be space-filling:

$$l_c = \phi_c d \qquad \text{and} \qquad l_a = (1 - \phi_c)d \tag{3}$$

The total scattering power, or invariant (Q), is related to the area beneath the Lorentz-corrected intensity function and is defined as:

$$Q = 1/(2\pi^2) \int_0^\infty i(q)q^2 \, dq \tag{4}$$

For an ideal two-phase system with sharp interfaces, then the invariant can be expressed as

$$Q = K\phi_c(1 - \phi_c)(\rho_c - \rho_a)^2 \tag{5}$$

where ρ_c and ρ_a are the electron densities of the crystalline and amorphous phases, respectively, and K is a constant related to the experimental geometry and the Thomson scattering factor. It is clear that changes in Q may arise from changes in crystallinity *or* from changes in the density difference between the phases.

In practice, the integration limits of 0 and ∞ in equation (4) are experimentally inaccessible and a precise value for Q must be obtained through the use of physically sensible extrapolation techniques. However, an adequate assessment of the magnitude of the invariant may be made[10] by integrating the background-subtracted curve of iq^2 *versus* q between the experimental q limits, q_1 and q_2.

An alternative approach for the characterization of lamellar morphologies involves the calculation of the one-dimensional correlation function[11–13], γ_1, which is essentially a one-dimensional Fourier transform of the SAXS intensity. γ_1 may be defined as:

$$\gamma_1(x) = \frac{\int_0^\infty i(q)q^2 \cos(qx) \, dq}{\int_0^\infty i(q)q^2 \, dq} \tag{6}$$

In lamellar systems, fluctuations in electron density only occur in a direction perpendicular to the plane of the lamellae. The correlation function, which is a mathematical restatement of the information contained in the SAXS pattern, provides a description of the variation in electron density as a function of distance within the sample. The interpretation of the correlation function is rather straightforward and allows direct evaluation of several structural features which describe the lamellar morphology. These include the d-spacing (or long period), the average thicknesses of the crystalline and amorphous layers, the (linear) crystallinity, the density difference between the two phases and the thickness of the interfacial region between the phases.

Previous SAXS studies have been performed on PHB and HV copolymer in order to investigate the morphology of single crystal mats[14,15] and melt-crystallized spherulites[16] as a function of crystallizer temperature and copolymer content. These studies were generally limited to the determination of long period spacings using lengthy, room temperature measurements on conventional X-ray sources. The high intensity of a synchrotron X-ray source enables SAXS patterns to be recorded in timescales of 10 s or less and allows simultaneous SAXS and d.s.c. measurements to be performed *in situ* during heating, melting or crystallization; such measurements are able to provide an insight into the morphological changes which are responsible for the complex d.s.c. behaviour observed in these polymers. Whislt the homopolymer has, under normal conditions, a single melting endotherm, the copolymers show multiple melt endotherms. The behaviour becomes increasingly complex as HV content increases, and as many as five separate peaks have been found for a 23% HV copolymer[17].

Multiple d.s.c. endotherms are found in several synthetic polymer systems. Linear low-density polyethylenes (LLDPEs) are structurally analogous to PHB–HV copolymers and consist of copolymers of ethylene with an α-olefin (e.g. propene-1-hexane); the comonomer units exist as short side branches on the main chain and affect the thickness and perfection of the crystalline lamellae as well as the overall crystallinity. LLDPEs exhibit several melting endotherms[18] which have been explained in terms of a heterogeneous distribution of crystal compositions which subsequently melt at different temperatures. Double melting endotherms in poly(ether ether ketone) (PEEK) and poly(ethylene terephthalate) (PET) homopolymers are the subject of some debate[19–26] and have been associated with two separate hypotheses: the two endotherms are either related to two distinct, pre-existing crystal morphologies or to a continuous melting and recrystallization phenomenon (which is characteristic of the crystallization history of the sample).

Recent studies of the melting behaviour of PEEK[27,28] have used time-resolved synchrotron SAXS techniques to investigate the structural changes which are associated with the d.s.c. endotherms. In both cases, it was concluded that the additional melting peaks are caused by the melting of thin, unstable crystals within the lamellar stacks, although the possibility of the thickening of the remaining lamellae during heating was also reported[28].

In previous d.s.c. studies of PHB and PHB–HV, multiple endotherms were attributed to the melting of different crystal populations with varying stabilities[14,15,17]. In particular, the occurrence of certain high temperature endotherms for HV copolymer samples has been associated with the possibility of a PHB-rich phase or the exclusion of HV units from the crystal lamellae.

The aim of this current work was to obtain an improved understanding of the structural changes which occur during the heating and melting of PHB and PHB/HV polymers, and to study the morphological features

Table 1 G.p.c. molecular weight data for the samples investigated

HV (%)	Annealing temp. (°C)	Annealing time (h)	$M_w \times 10^{-3}$
0	40	72	274
	60	20	351
	80	24	239
	100	45	323
7	40	72	201
	60	20	117
	80	24	135
	100	45	227
10	80	15	286
19	40	72	383
	60	20	235
	80	24	263
	100	45	278

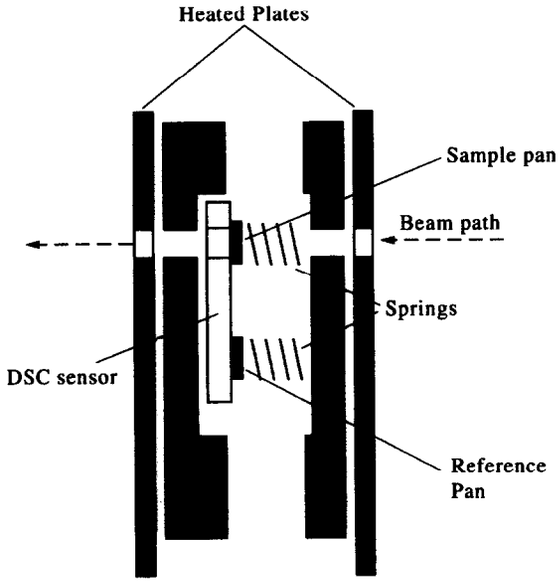

Figure 1 Modified hot-stage differential scanning calorimeter used for elevated temperature measurements

and the modification of physical properties which are associated with the multiple d.s.c. endotherms.

EXPERIMENTAL

Sample preparation

Polymers of 0, 7, 10 and 19% HV were chosen for investigation. All samples were prepared as sheets of approximate thickness 0.5 mm by compression moulding. The plaques were formed at 175°C under 3 tonne cm^{-2}, then quenched directly from the press into iced water. The amorphous material thus produced was then crystallized at the required temperature by placing it in an oven between preheated metal plates. Molecular weights of the crystallized plaques are given in *Table 1*.

Gel permeation chromatography (g.p.c.)

G.p.c. was used to determine the M_w of the compression moulded and annealed plaques. Chromatograms were obtained at 30°C in chloroform using a Knauer Instruments apparatus equipped with a set of two 10 μm Polymer Labs mixed gel columns (300 × 7.5 mm) and a Foxboro Miran 1A infra-red detector. The system was calibrated using monodisperse polystyrene standards and ethyl acetate was used as an internal calibrant. Data analyses were performed on a BBC Master computer using a Polymer Labs software package and utilizing the known Mark–Houwink parameters for polystyrene[29] and PHB[30].

Small-angle X-ray scattering

SAXS measurements were performed using station 2.1 of the SRS at the SERC Daresbury Laboratory, Warrington, UK, which possesses a highly intense, monochromatic beam of wavelength 1.54 Å. The beam was collimated to cross-sectional dimensions of approximately 2 × 1 mm and the scattered X-rays were recorded on a multiwire detector located around 2.5 m behind the sample in a simple transmission geometry. A Mettler hot-stage differential scanning calorimeter, modified by ICI for X-ray scattering experiments at the SRS, was used for all elevated temperature measurements. The hot-stage sat upright in the beam path and possessed holes before and after the sample thorough which the beam could pass (see *Figure 1*). Circular windows were punched in the lid and base of aluminium d.s.c. pans used to contain the samples, which were sandwiched between two 10 μm mica sheets.

The optimum sample thickness for X-ray scattering in the transmission configuration is generally considered to be $1/\mu$ (where μ is the linear X-ray absorption coefficient). For PHB, μ was calculated to be 8.4 cm^{-1} at a wavelength of 1.54 Å, giving a desired thickness of around 1.2 mm. Slightly thinner samples (0.5–0.1 mm) were used in the hot-stage in order to minimize temperature fluctuations across the sample. SAXS/d.s.c. measurements were performed on samples of PHB, 7% HV, 10% HV and 19% HV copolymer, each of which had been annealed at a temperature of 60 or 100°C. SAXS patterns were recorded continuously between 50–200°C using an exposure time of 20 s per frame; this provided a resolution of just over 3°C per frame using a standard d.s.c. heating rate of 10°C min^{-1}. The start of the first exposure was synchronized with the initial point in the d.s.c. trace in order to provide a temperature calibration of the SAXS patterns. A total of 45 patterns was recorded for each heating run.

In addition to the d.s.c. scans obtained using the modified Mettler hot-stage at Daresbury, better quality d.s.c. data were obtained by repeating the analyses on Perkin–Elmer DSC4 and DSC7 calorimeters. Scans were made at a heating rate of 10°C min^{-1} over the range 20 to 200°C using samples of the order of 10 mg. Both Perkin–Elmer calorimeters were calibrated with indium and the curves from them are comparable to within ±2°C.

The raw SAXS patterns were normalized to account for variations in X-ray absorption and incident beam flux using an ionization chamber located after the sample. Corrections were also made for the non-uniformity of response of the individual detector elements (using radiation from an ^{55}Fe source). The q-axis was calibrated using the known diffraction peak positions of wet rat-tail collagen.

Each data set was then calibrated to absolute scattering units[31] according to the value of the experimental scattering peak recorded from a known standard

material (Lupolen). The calibration factor also accounts for the variation in thickness from sample to sample. Absolute scaling enables quantitative comparisons to be made between different samples and experimental sessions and provides access to the actual electron density contrast between the crystalline and amorphous phases in the sample. Plots of Lorentz-corrected intensity (iq^2) as a function of q were calculated, allowing estimates of the Bragg long period and the relative invariant, Q, to be made.

A preliminary SAXS/d.s.c. investigation was performed using samples of PHB homopolymer, 7% HV copolymer and 19% HV copolymer, each of which had been annealed at a temperature of 60 or 100°C prior to the experiment. The SAXS patterns obtained during these experiments were adequate for the determination of Bragg spacings and relative invariants and establishment of the general features of the behaviour of each material. However, the calculation of one-dimensional correlation functions was not attempted since the limited range of the detector prevented the observation of a sufficiently smooth 'tail' to allow reliable extrapolations of the data to be made. A more detailed experiment was subsequently performed using a 10% HV copolymer which involved a thorough investigation of the structure of the material close to melting and also allowed the calculation of time-resolved correlation functions during heating.

In addition to these time-resolved experiments, 'static' SAXS patterns were recorded at room temperature and at fixed, elevated temperatures for several samples of PHB and HV copolymer to investigate the influence of annealing temperature upon the lamellar morphology.

RESULTS

D.s.c. traces for each of the six samples in the preliminary SAXS/d.s.c. experiments are reproduced in *Figure 2*. In broad terms, the homopolymer samples were found to possess a single melting endotherm whilst the copolymer samples possessed a double endotherm in which the position and prominence of the minor peak varied with the annealing temperature of the sample. Each of the six samples exhibited a shoulder (or change in slope) in its d.s.c. trace close to the original annealing temperature. These shoulders are most obvious in the copolymer samples annealed at 100°C.

A general impression of the change in the SAXS pattern as a function of temperature during the course of these experiments is provided in *Figure 3*, which illustrates the evolution of the SAXS intensity with increasing temperature during the heating of one of the HV copolymer samples. In fact, the overall behaviour of each of the materials was remarkably similar. As shown in *Figure 3*, the SAXS correlation peak was found to grow in intensity at a fairly steady value of q_{max} during the early stages of heating; subsequently, the peak position shifted dramatically to lower q (equivalent to higher characteristic long period spacing). On the point of melting, a highly intense, peakless, monotonically decreasing scattering pattern was briefly observed. Finally, the scattering disappeared as the sample became completely molten. Owing to the shift in peak position during the later stages of heating, the *i versus q* plot exhibited an enormous increase in peak intensity; however, the

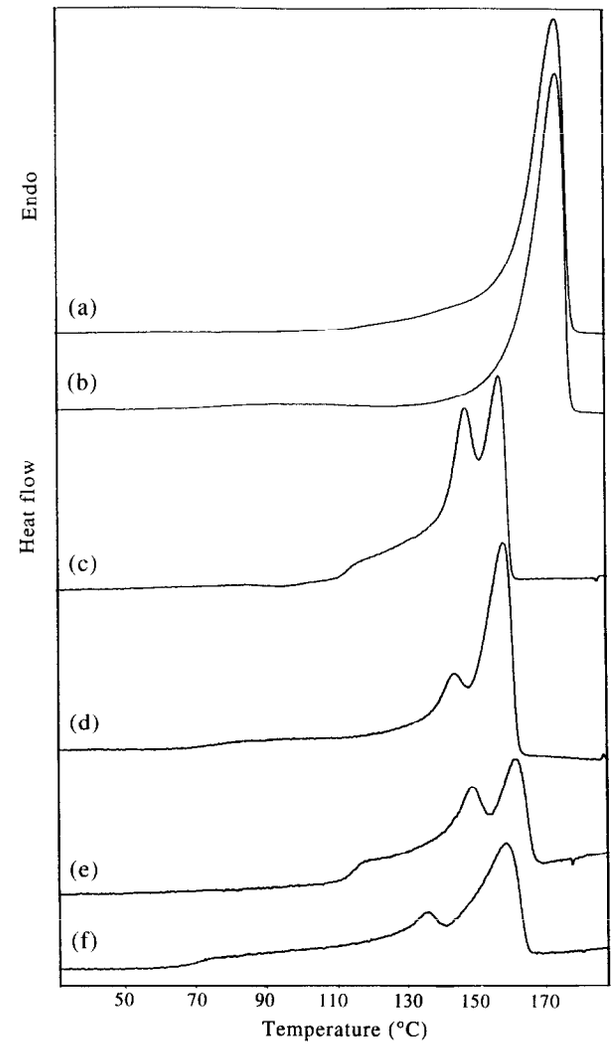

Figure 2 Perkin–Elmer d.s.c. curves obtained for the samples examined at Daresbury: (A) 0% HV, annealed 100°C; (B) 0% HV, annealed 60°C; (C) 7% HV, annealed 100°C; (D) 7% HV, annealed 60°C; (E) 19% HV, annealed 100°C; (F) 19% HV, annealed 60°C

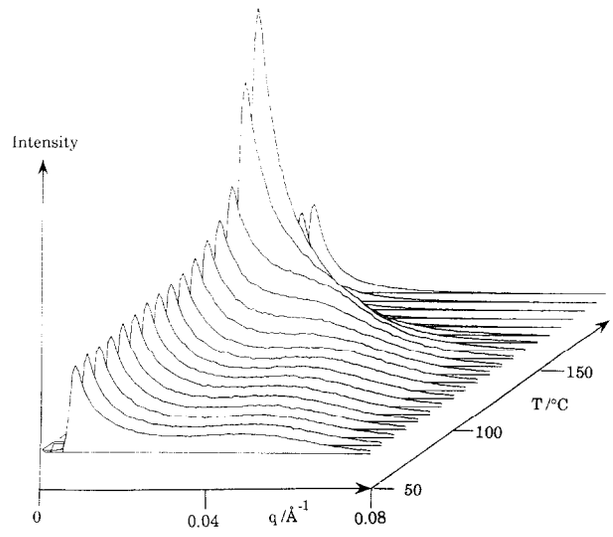

Figure 3 Evolution of SAXS intensity as a function of temperature for 19% HV copolymer sample (annealed at 100°C). Exposure time 20 s per pattern, heating rate 10°C min^{-1}

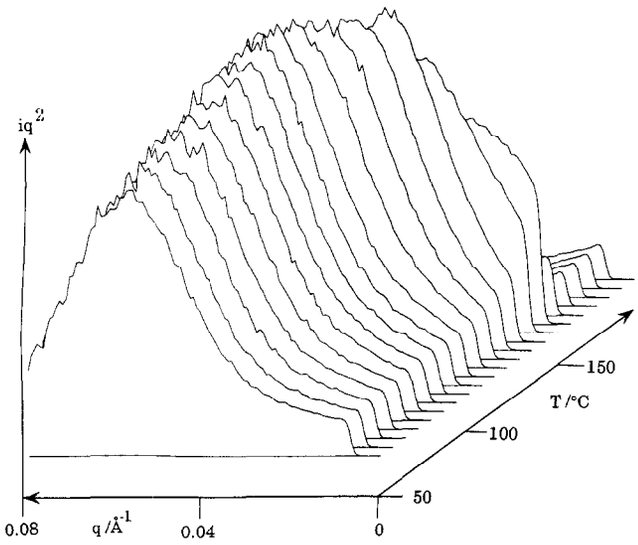

Figure 4 Changes in the Lorentz-corrected (iq^2 *versus* q) SAXS pattern as a function of temperature for 19% HV copolymer sample (annealed at 100°C)

Lorentz-corrected plots, which are shown in *Figure 4*, maintained a reasonably constant peak height during this rapid change in peak position.

Figure 5 shows the variation in long period d with temperature, as calculated from the positions of the maxima in the Lorentz-corrected plots. In each case, a sharp change in the rate of increase of d can be seen at around 135°C. Below this value, the long period of the samples annealed at 60°C rose more rapidly than that of the samples annealed at 100°C; above this value, the behaviour of any given material appeared to be independent of its annealing temperature. Measurable values for d were obtained up to temperatures of about 170°C for PHB and about 150°C for the copolymers.

In each of the six samples, the variation in d with temperature was fairly smooth and continuous. In some other materials which exhibit multiple endotherms, a stepwise increase in d has been observed during heating in which each step coincided with a peak in the d.s.c. trace[27]. The occurrence of discontinuous steps in the behaviour of d provides strong evidence for the existence within the material of distinct populations of crystals with different stabilities.

The behaviour of the invariant as a function of temperature is shown in *Figure 6* for each of the six samples studied. In each case, two distinct regions are apparent: in the early stages, the invariant rises steadily and, beyond the onset of melting, the invariant falls rapidly. Any attempt to interpret the heating and melting behaviour of PHB and HV copolymer in the light of this information alone is complicated by several factors. The invariant is governed by contributions from two different physical parameters, i.e. the crystallinity (ϕ) and the electron density contrast ($\rho_c - \rho_a$), which are difficult to distinguish without further information. The electron density contrast term is known to increase as a result of thermal expansion; however, it may also change as a result of structural modifications in the copolymer crystals (e.g. exclusion of HV units). Consequently, no significant conclusions will be drawn from the behaviour of the invariant with temperature, which has been

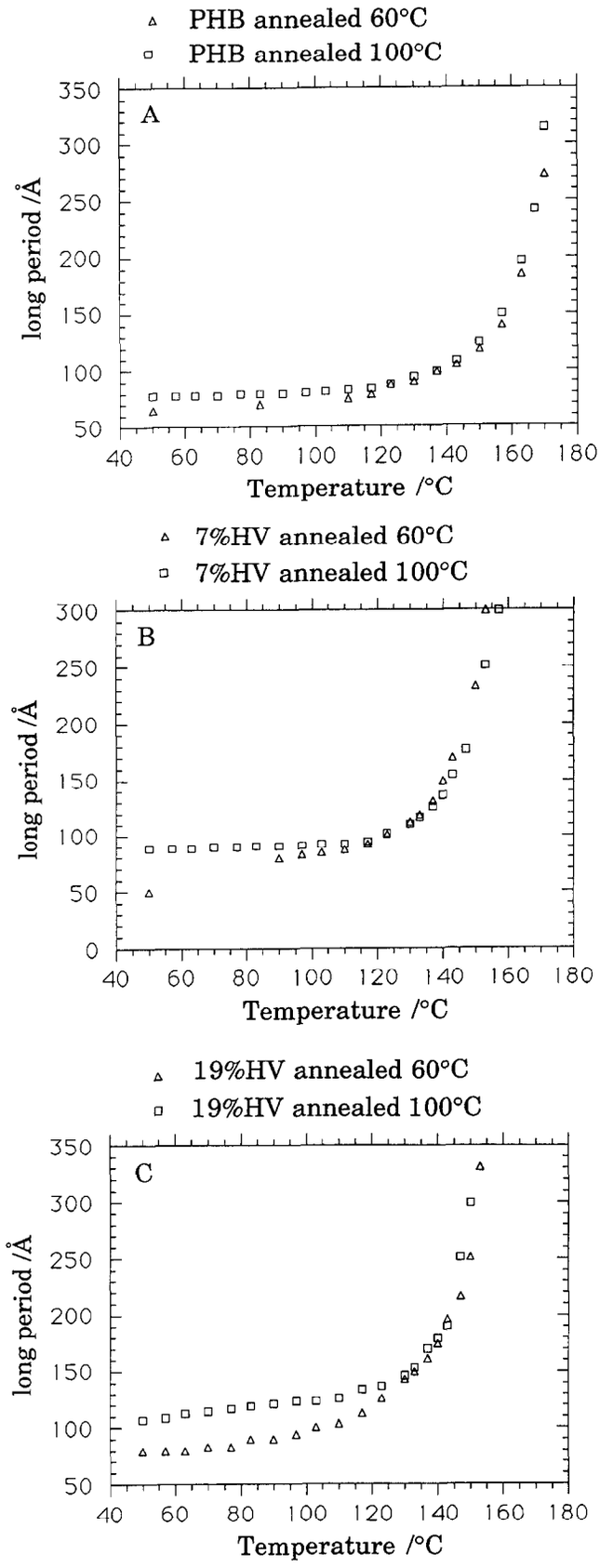

Figure 5 Variation in long period spacing as a function of temperature for PHB (A), 7% HV copolymer (B) and 19% HV copolymer (C)

observed in numerous experiments for several materials (see, for example, refs 18, 27, 28 and 32). However, it is clear that the use of simultaneous small- and wide-angle measurements (SAXS/WAXS)[27,32] would be beneficial in

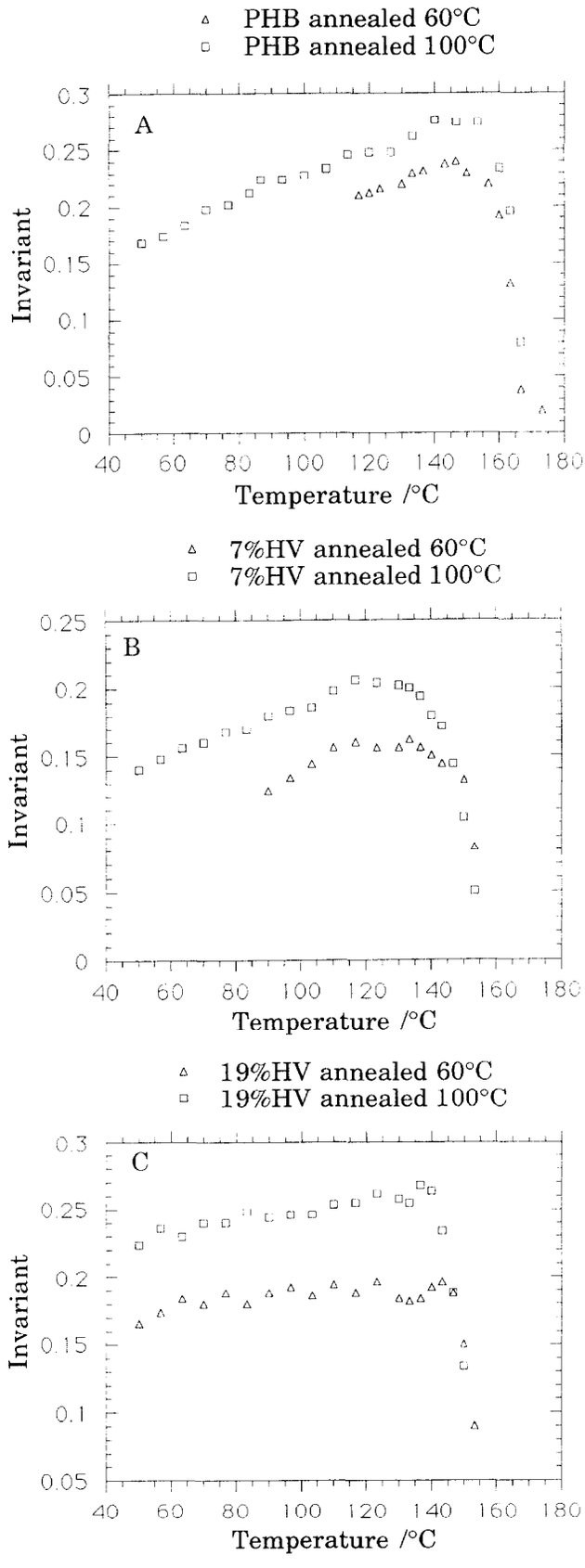

Figure 6 Variation in the SAXS invariant as a function of temperature for PHB (A), 7% HV copolymer (B) and 19% HV copolymer (C)

providing an independent measurement of crystallinity throughout the heating process.

A more interesting feature of these experiments is the occurrence of an intense, monotonically decreasing

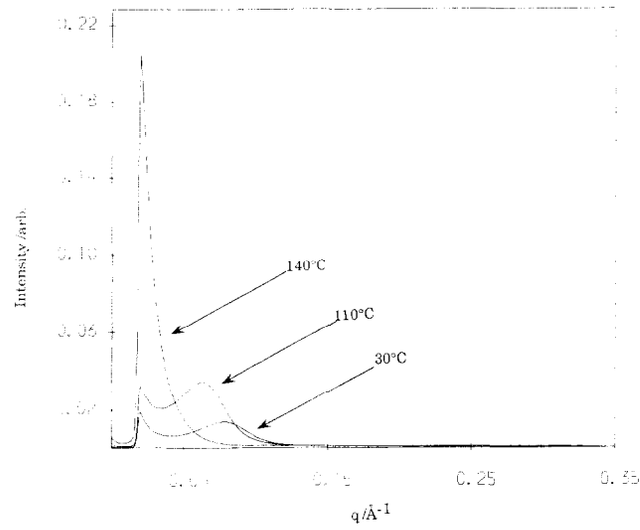

Figure 7 Appearance of SAXS pattern (*i versus q*) at selected temperatures for 10% HV copolymer

scattering pattern close to melting. This feature is evident in *Figure 3* but is shown in greater detail for a 10% HV copolymer in *Figure 7*. In certain respects, this type of pattern could be considered to be the tail of a correlation peak which has shifted to very low values of q, obscured by the beamstop (if this were the case, then the typical separation of neighbouring lamellae would be extremely large). However, considered in isolation, such a smoothly decreasing intensity function would not normally be associated with a regular morphology, although the level of scattering is still fairly high (indicating that significant heterogeneities are still present). Thus it is more reasonable to interpret this scattering feature as arising from isolated crystalline lamellae which are widely dispersed in a disordered matrix.

A common form of analysis which is invoked in the case of such 'dilute' assemblies is the Guinier approximation. In the case of lamellae, which are assumed to exist in PHB and HV copolymers even close to melting, the Guinier approximation is given by[8]:

$$iq^2 = Ct^2 \exp(-R_t^2 q^2) \tag{7}$$

where R_t is the cross-sectional radius of gyration related to a disc-like morphology and t is the disc thickness (or in this approximate case, the lamellar thickness). This is a modification of the standard Guinier law and holds well for monodisperse particles at small values of q ($<1/R_t$). A plot of $\ln(iq^2)$ *versus* q^2 yields R_t from its slope. The lamellar thickness is easily calculated, since

$$t = \sqrt{12} R_t \tag{8}$$

Cross-sectional Guinier plots of $\ln(iq^2)$ *versus* q^2 were obtained for each of the six samples discussed earlier using the low q portion of the monotonically decreasing SAXS pattern close to melting. One such plot is shown in *Figure 8*. A reasonable linear dependence was obtained for each sample and values of the lamellar thickness were calculated from the slope of each plot. These values are tabulated in *Table 2*.

For each sample, the calculated lamellar thickness close to melting was greater than the average thickness at room temperature (estimated to lie between 48 and 60 Å

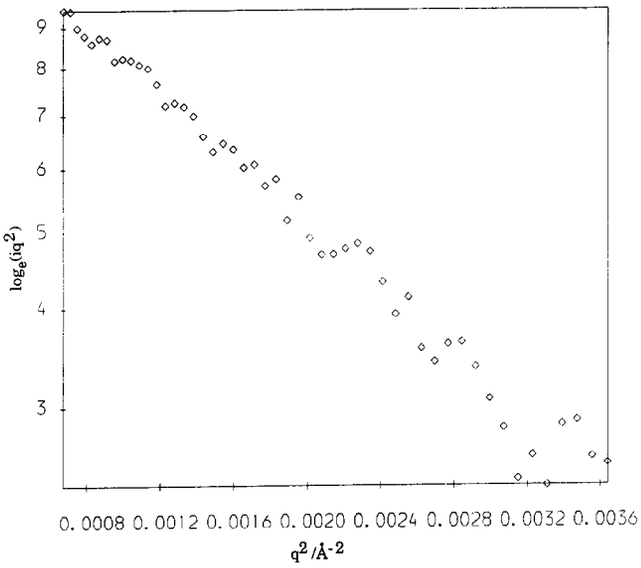

Figure 8 Typical cross-sectional Guinier plot [$\ln(iq^2)$ *versus* q^2] derived from SAXS pattern close to melting (example 19% HV copolymer, 100°C annealed, sample temperature 150°C)

Table 2 Lamellar thicknesses close to melting as determined by Guinier analysis

	Annealing temp. (°C)	Lamellar thickness (Å)
PHB	60	101
	100	103
7% HV copolymer	60	73
	100	74
19% HV copolymer	60	74
	100	74

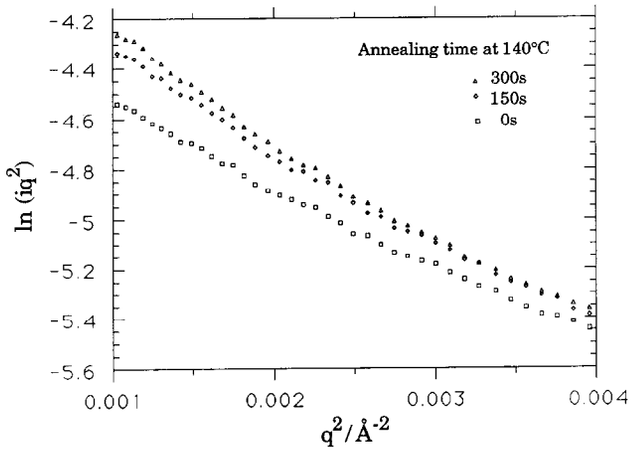

Figure 9 Series of cross-sectional Guinier plots [$\ln(iq^2)$ *versus* q^2] for 10% HV copolymer maintained at high temperature close to melting (140°C)

for all samples). This observation confirms that the thicker, more stable lamellae are the last to melt. It is also apparent that the thicknesses of the homopolymer lamellae close to melting are substantially larger than those of the copolymer samples. This would appear to suggest that the presence of the HV units in the copolymer limit, or constrain, the thickness of the crystalline lamellae.

Further experiments were performed on a 10% HV

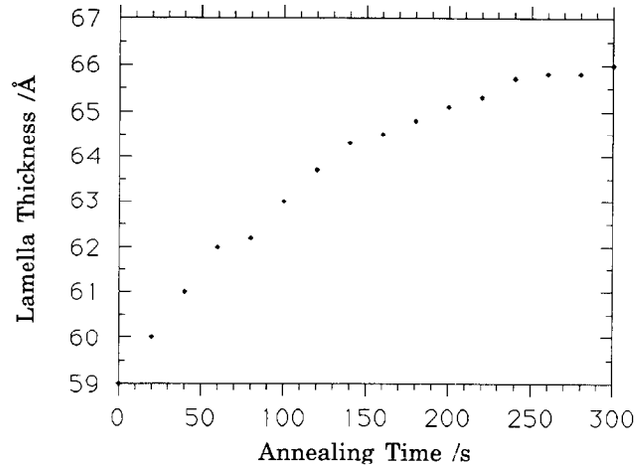

Figure 10 Variation in lamellar thickness for 10% HV copolymer maintained at high temperature close to melting (140°C)

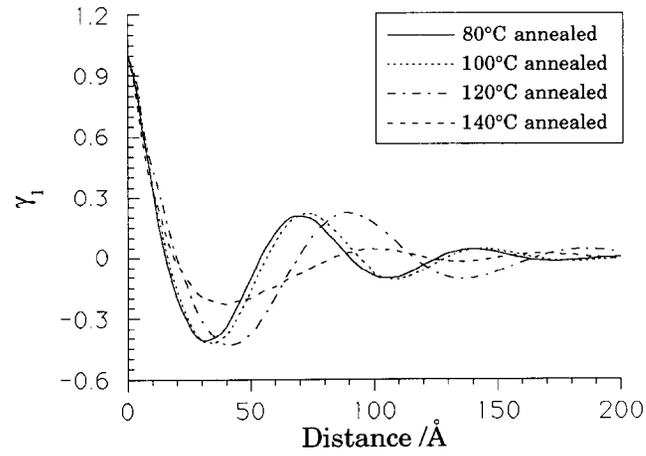

Figure 11 One-dimensional correlation functions obtained at room temperature from samples of 10% HV copolymer annealed at temperatures of 80, 100, 120 and 140°C

copolymer to assess the behaviour of the lamellar thickness when the material is annealed at a temperature close to its melting point. A sample of 10% HV copolymer was heated to 140°C, which is higher than the first endotherm in the d.s.c. trace, and maintained at this temperature for a period of 5 min. As shown in *Figure 7*, the SAXS pattern at this temperature consists of an intense, peakless scattering feature close to the origin. During annealing at 140°C, SAXS patterns were recorded at intervals of 20 s and small variations in the slope and magnitude of this intense scattering feature were observed. Cross-sectional Guinier plots were obtained from each of these SAXS patterns and a selection of these plots is provided in *Figure 9*.

The lamellar thickness was calculated from the slope of each plot and was found to increase steadily during the annealing process, as illustrated in *Figure 10*. This observation suggests that the remaining lamellae are capable of thickening during heating at temperatures approaching the final melting point. The increase in the lamellar thickness was more rapid during the early stages of annealing, immediately after the sample reached the temperature of 140°C.

To investigate the influence of annealing temperature upon lamellar thickness, SAXS patterns were obtained

Table 3 Morphological parameters of samples of 10% HV copolymer annealed at different temperatures

Annealing temp. (°C)	Long period (Å)	Crystal thickness (Å)	Amorphous thickness (Å)
80	70	46	24
100	74	49	25
120	89	59	30
140	98	74	24

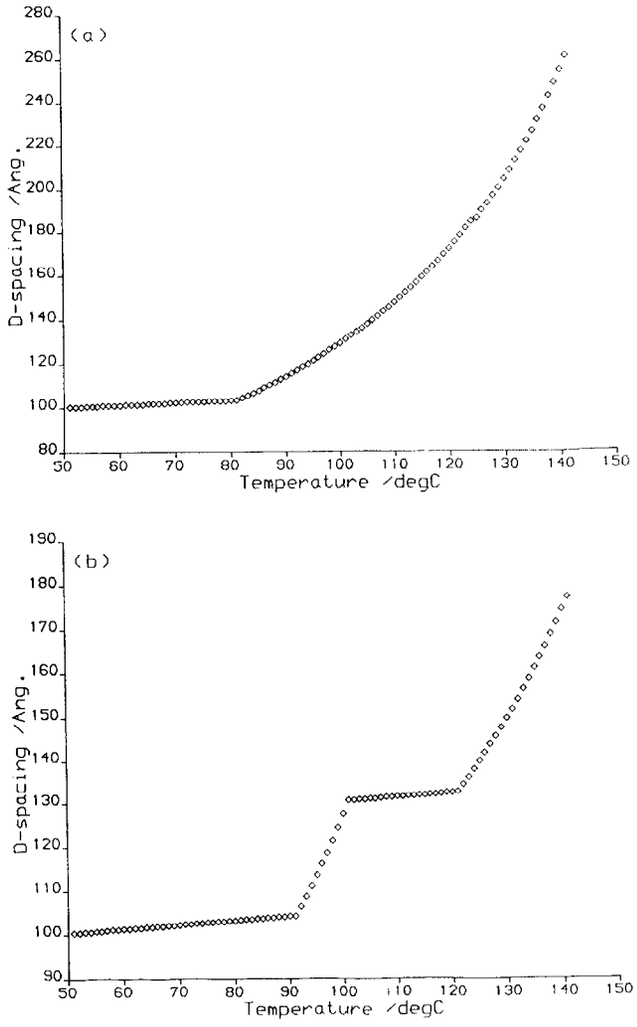

Figure 12 Simulations of the variation in the average long period of a simple lamellar stack model as the result of: (a) a continuous melting process; (b) a stepwise melting process

(at room temperature) from several samples of 10% HV copolymer which had been annealed at temperatures of 80, 100, 120 and 140°C for periods of 1 h or more. One-dimensional correlation functions obtained from these SAXS patterns indicated that, rather predictably, the lamellar thickness increased with annealing temperature. The correlation functions are reproduced in *Figure 11* and the results are summarized in *Table 3*.

It is interesting to note that the samples annealed at 140°C displayed an average lamellar thickness (after cooling to room temperature) of 74 Å. This value corresponds well with the values obtained from the time-resolved Guinier analysis of the SAXS patterns during annealing at 140°C. It would be anticipated that the samples which were annealed for a significant length of time would be more likely to approach the equilibrium morphology and would possess larger lamellar thicknesses than those observed during the real-time annealing process.

DISCUSSION

The general behaviour of the SAXS pattern obtained from PHB and HV copolymer during heating and melting has been observed before in several semicrystalline polymers possessing lamellar morphologies. The initial rise in intensity and the associated increase in the invariant are consistent with thermal expansion effects. The subsequent shift of the scattering peak to lower q values with the onset of melting is also well understood and arises from the melting of thin, unstable lamellae within the lamellar stacks. The disappearance of these lamellae produces an increase in the average separation between neighbouring lamellae; hence the long period increases and the scattering peak moves to lower q. In the case of PHB, the possibility of lamellar thickening[33] during the early stages of heating cannot be ruled out on the basis of the data presented here. The relative contributions of lamellar thickening and/or melting to the changing morphology during heating are dependent on several factors, including the thermal history of the sample and the heating rate. However, the effect of lamellar thickening upon the long period is not as dramatic as the effect of melting[34].

The behaviour of the long period during melting provides a simple but useful indicator of the changing morphology of the sample. In studying the melting behaviour of PEEK, which also exhibits multiple d.s.c. endotherms, Kruger and Zachmann[27] observed a stepwise increase in the long period during heating in which each step coincided with a peak in the d.s.c. trace. The occurrence of discrete steps in the behaviour of the long period was associated with the disappearance of separate populations of crystals, each possessing different thicknesses and stabilities. In the case of PHB and HV copolymer, the long period was found to increase steadily throughout heating and there were no apparent discontinuities which could be related to the separate endotherms in the d.s.c. trace. This seems to suggest that the distribution of lamellar thicknesses in PHB and HV copolymer is so broad that the features of the d.s.c. trace cannot be associated directly with the disappearance of any distinct populations of lamellae.

A simple computer model was constructed to simulate the observed change in d-spacing during heating. The model consisted of a large stack of crystalline lamellae in which the separation of neighbouring lamellae took the form of a Gaussian distribution about the mean long period. The melting process was simulated by the sequential removal of individual lamellae, selected at random from the stack, followed by a recalculation of the mean long period. The number of units removed at any given stage could be varied in order to reproduce the different rates of melting at different temperatures. As such, the thickness distribution was determined by the number of lamellae removed at any given temperature during the simulated heating process.

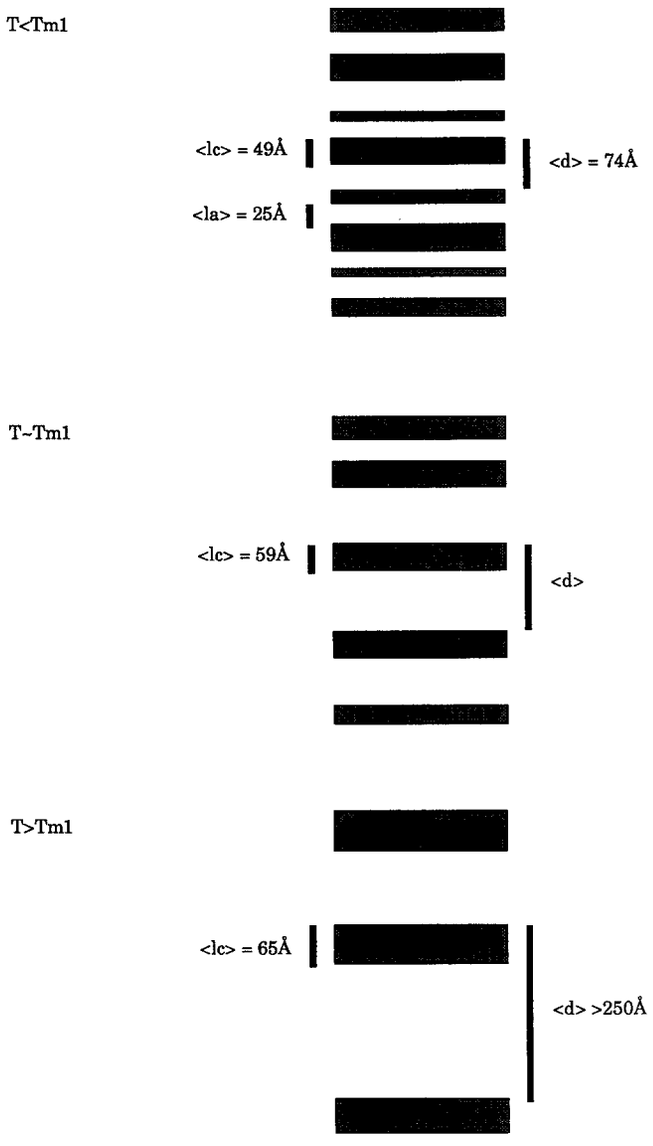

Figure 13 Schematic illustration of the change in morphology of 19% HV copolymer as quantified by correlation function analysis and Guinier analysis during heating and melting (after Hsaio *et al.*[28])

It was found that, in order to reproduce the steady increase in the long period which is observed for PHB and HV copolymer, it was necessary to invoke a continuous melting behaviour. This was achieved by removing a constant number of lamellae for each rise in temperature during the simulation. This mimics a broad distribution of lamellar thicknesses and predicts a steady rise in *d*-spacing during heating, as shown in *Figure 12a*. Discontinuities in the behaviour of the long period could be introduced by removing lamellae in separate steps, as if distinct populations of crystals were present in the material. The result of a simulation in which lamellae were removed in two separate stages during heating is shown in *Figure 12b*. Naturally, this basic model does not attempt to include the more complex phenomena such as surface melting[35], but provides a useful starting point for understanding the observed SAXS behaviour.

In fact, the d.s.c. behaviour of PHB and HV copolymers was different to that of homopolymers such as PEEK since the multiple endotherms were only observed in the case of the copolymer. It is clear that some characteristic of the copolymer crystals enables a larger number of thin, unstable crystals to form, which melt at an early stage during heating. It is possible that during the primary crystallization of the copolymer, the lamellae are constrained in some way from thickening and the subsequent (secondary) crystallization introduces a larger proportion of thin, infilling lamellae within the lamellar stacks. The copolymer crystals are probably constrained either as a result of HV inclusion (which introduces a crystal 'defect' and reduces the enthalpy of fusion of the crystal) or a result of increased surface energy. Indeed, it is interesting to note that the homopolymer lamellar thicknesses derived from the Guinier analysis close to melting are consistently larger than the copolymer lamellae, irrespective of sample annealing history.

It is clear that the melting of HV copolymer involves the gradual disappearance of thin lamellae which are presumed to exist in the domains separating the primary lamellae. The distribution of lamellar thicknesses and separation are very large and no discontinuities are apparent in the SAXS behaviour. The remaining lamellae are able to anneal at temperatures close to melting assisted by the increased thermal motion of the polymer chains. The ability of the time-resolved measurements to follow (and quantify) the thickening process provides an intriguing insight into the behaviour of the polymer immediately prior to melting. The change in the morphology throughout the entire melting process may be quantified, and is illustrated schematically for a 19% HV copolymer in *Figure 13*, which is based on the description of the melting of PEEK by Hsaio *et al.*[28].

CONCLUSIONS

Time-resolved SAXS data from PHB and HV copolymer during heating and melting indicates a peak which moves to lower q with increasing temperature. This behaviour has been interpreted in terms of the progressive melting of unstable crystalline lamellae within the lameller stacks. A smooth, continuous change in *d*-spacing has been observed for both PHB and HV copolymer during melting, which has been shown to be associated with the melting of crystals possessing a broad range of thicknesses. A simple model has been used to illustrate the discontinuous behaviour which would otherwise be anticipated if the sample consisted of discrete populations of lamellae with distinctly different stabilities.

Clear differences are apparent between the d.s.c. behaviour of PHB homopolymer and PHB–HV copolymer, which have been associated with a difference in crystal thicknesses for the homopolymer and copolymer at any given temperature. This difference is not only associated with the different undercoolings for each material but also with the effect of the HV units in raising the surface energy of the crystal. However, the values of the lamellar thicknesses obtained by correlation function analysis and Guinier analysis close to melting are so large that HV units are statistically unlikely to be excluded from the crystals.

The changing morphology immediately prior to melting has been characterized by a Guinier analysis of the intense peakless SAXS feature. This has provided evidence for a gradual thickening of the remaining

isolated lamellae during heating or annealing. This thickening (or recrystallization) phenomenon appears to be more prevalent in the copolymer case, giving rise to the multiple endotherms in the d.s.c. The use of combined SAXS/WAXS could provide a further insight into the possible crystal structure changes which are associated with the lamellar thickening phenomenon in the copolymer and the multiple d.s.c. endotherms.

REFERENCES

1 Mergaert, J., Anderson, C., Wouters, A., Swings, J. and Kesters, K. *FEMS Microbiol. Rev.* 1992, **103**, 317
2 Kemmish, D. J. in 'Biogradable Plastics & Packaging' (Eds C. Ching, D. L. Kaplan and E. L. Thomas), Technomic, Lancaster, PA, 1993
3 Davies, E. A. and Senior, P. J. *Adv. Microb. Physiol.* 1973, **10**, 135
4 Byrom, D. *Trends in Biotechnol.* 1987, **5**, 246
5 Bluhm, T. L., Hamer, G. K., Marchessault, R. H., Fyfe, C. A. and Veregin, R. P. *Macromolecules* 1986, **19**, 2871
6 Kunioka, M., Tamaki, A. and Doi, Y. *Macromolecules* 1989, **22**, 694
7 Scandola, M., Ceccorulli, G., Pizzoli, M. and Gazzano, M. *Macromolecules* 1992, **25**, 1405
8 Glatter, O. and Kratky, O. (Eds) 'Small Angle X-ray Scattering'. Academic Press, London, 1982
9 Balta-Calleja, F. J. and Vonk, C. G. 'X-ray Scattering of Synthetic Polymers', Elsevier, Amsterdam, 1989, Polymer Science Library
10 Vonk, C. G. *J. Appl. Cryst.* 1973, **6**, 81
11 Vonk, C. G. and Kortleve, G. *Koll. Z. Z. Polym.* 1967, **220**, 19
12 Vonk, C. G. *J. Appl. Cryst.* 1971, **4**, 340
13 Strobl, G. R. and Schneider, M. J. *J. Polym. Sci., Polym. Phys. Edn* 1980, **18**, 1343
14 Mitomo, H., Barham, P. J. and Keller, A. *Polym. J.* 1987, **19**, 1241
15 Mitomo, H., Barham, P. J. and Keller, A. *Seni-Gakkaishi* 1986, **42**, T589
16 Barham, P. J., Keller, A., Otun, E. L. and Holmes, P. A. *J. Mater. Sci.* 1984, **19**, 2781
17 Organ, S. J. and Barham, P. J. *J. Mater. Sci.* 1991, **26**, 1368
18 Schouterden, P., Vandermarliere, M., Riekel, C., Koch, M. H. J., Groeninckx, G. and Reynaers, H. *Macromolecules* 1989, **22**, 237
19 Blundell, D. J. and Osborn, B. N. *Polymer* 1983, **24**, 253
20 Blundell, D. J. *Polymer* 1987, **28**, 2248
21 Cebe, P. and Hong, S. D. *Polymer* 1986, **27**, 1183
22 Lee, Y. and Porter, R. S. *Macromolecules* 1987, **20**, 1336
23 Lee, Y., Porter, R. S. and Lin, J. S. *Macromolecules* 1989, **22**, 1756
24 Bassett, D. C., Olley, R. H. and Al Raheil, I. A. M. *Polymer* 1988, **29**, 1945
25 Bell, J. P. and Murayama, R. *J. Polym. Sci. A2* 1969, **7**, 1059
26 Roberts, R. C. *Polymer* 1969, **10**, 117
27 Kruger, K.-N. and Zachmann, H. G. *Macromolecules* 1993, **26**, 5202
28 Hsaio, B. S., Gardner, K. H., Wu, D. Q. and Chu, B. *Polymer* 1993, **34**, 3996
29 Brandrup, J. and Immergut, E. H. 'Polymer Handbook', 3rd edn, Wiley, Somerset, NJ, 1989
30 Atika, S., Eindga, Y., Miyaki, Y. and Fukita, H. *Macromolecules* 1976, **9**, 774
31 Russell, T. P., Lin, J. S., Spooner, S. and Wignall, G. D. *J. Appl. Cryst.* 1988, **21**, 629
32 Bras, W., Derbyshire, G. E., Ryan, A. J., Mant, G. R., Felton, A., Lewis, R. A., Hall, C. J. and Greaves, G. N. *Nucl. Instrum. Meth. Phys. Res.* 1993, **A326**, 587
33 De Konig, G. J. M. *PhD Thesis*, Eindhoven University of Technology, 1993
34 Zachmann, H. G. and Wutz, C. in 'Crystallisation of Polymers' (Ed. M. Dosiere), Kluwer, The Netherlands, 1993, p. 404
35 Fischer, E. W. *Kolloid Z. Z. Polym.* 1967, **218**, 97